

Article

Mid-IR Optical Property of Dy:CaF₂-SrF₂ Crystal Fabricated by Multicrucible Temperature Gradient Technology

Lihe Zheng¹, Jianbin Zhao¹, Yangxiao Wang², Weichao Chen^{3,*}, Fangfang Ruan^{4,*}, Hui Lin⁵, Yanyan Xue⁶, Jian Liu⁶, Yang Liu¹, Ruiqin Yang¹, Haifeng Lu¹, Xiaodong Xu⁷ and Liangbi Su²

- ¹ Key Laboratory of Yunnan Provincial Higher Education Institutions for Optoelectronics Device Engineering, School of Physics and Astronomy, Yunnan University, Kunming 650500, China; zhenglihe@ynu.edu.cn (L.Z.); jianbinzhao@mail.ynu.edu.cn (J.Z.); liuyang1@mail.ynu.edu.cn (Y.L.); yangruiqin@mail.ynu.edu.cn (R.Y.); 2943277027@mail.ynu.edu.cn (H.L.)
 - ² Key Laboratory of Transparent Opto-functional Inorganic Materials, Shanghai Institute of Ceramics, Chinese Academy of Sciences, Shanghai 201899, China; wangtim@student.sic.ac.cn (Y.W.); suliangbi@sic.ac.cn (L.S.)
 - ³ School of Technology, Pu'er University, Pu'er 665000, China
 - ⁴ Department of Medical Imaging, Hangzhou Medical College, Hangzhou 310053, China
 - ⁵ Engineering Research Center of Optical Instrument and System, Ministry of Education and Shanghai Key Lab of Modern Optical System, University of Shanghai for Science and Technology, Shanghai 200093, China; linh8112@163.com
 - ⁶ School of Physics Science and Engineering, Tongji University, Shanghai 200092, China; xueyanyan@163.com (Y.X.); 1910102@tongji.edu.cn (J.L.)
 - ⁷ Jiangsu Key Laboratory of Advanced Laser Materials and Devices, School of Physics and Electronic Engineering, Jiangsu Normal University, Xuzhou 221116, China; xdxu79@jsnu.edu.cn
- * Correspondence: weichaochen2010@foxmail.com (W.C.); ruan.f@hmc.edu.cn (F.R.)



Citation: Zheng, L.; Zhao, J.; Wang, Y.; Chen, W.; Ruan, F.; Lin, H.; Xue, Y.; Liu, J.; Liu, Y.; Yang, R.; et al. Mid-IR Optical Property of Dy:CaF₂-SrF₂ Crystal Fabricated by Multicrucible Temperature Gradient Technology. *Crystals* **2021**, *11*, 907. <https://doi.org/10.3390/cryst11080907>

Academic Editors: Ludmila Isaenko, Xiaoming Duan, Renqin Dou, Linjun Li and Xiaotao Yang

Received: 1 July 2021

Accepted: 27 July 2021

Published: 31 July 2021

Publisher's Note: MDPI stays neutral with regard to jurisdictional claims in published maps and institutional affiliations.



Copyright: © 2021 by the authors. Licensee MDPI, Basel, Switzerland. This article is an open access article distributed under the terms and conditions of the Creative Commons Attribution (CC BY) license (<https://creativecommons.org/licenses/by/4.0/>).

Abstract: Dy³⁺-doped CaF₂-SrF₂ crystals with various Dy³⁺ dopant concentrations were synthesized by multicrucible temperature gradient technology (MC-TGT). Dy:CaF₂-SrF₂ crystals were fluorite structured and crystallized in cubic *Fm* $\bar{3}$ *m* space group, as characterized by X-ray diffraction. The crystallographic site concentration was calculated from the measured density by Archimedes' hydrostatic weighing principle. The optical transmission reached over 90% with a sample thickness of 1.0 mm. The Sellmeier dispersion formula was obtained following the measured refractive index in a mid-IR range of 1.7–11 μ m. Absorption coefficients of 6.06 cm⁻¹ and 12.71 cm⁻¹ were obtained at 804 nm and 1094 nm in 15% Dy:CaF₂-SrF₂ crystal. The fluorescence spectra of 15 at.% Dy:CaF₂-SrF₂ showed the strongest wavelength peak at 2919 nm with a full width at half maximum (FWHM) of 267 nm under an excitation wavelength of 808 nm. The fluorescence lifetimes were illustrated for different Dy³⁺ dopant levels of 5%, 10% and 15%. The results indicate that the Dy:CaF₂-SrF₂ crystal is a promising candidate for compact mid-IR lasers.

Keywords: Dy:CaF₂-SrF₂; crystal growth; temperature gradient technology; midinfrared crystal; Sellmeier dispersion formula

1. Introduction

Midinfrared (mid-IR) lasers are considered of great importance due to their wide applications in fundamental and practical fields such as directional infrared countermeasures, atmospheric monitoring, biomedicine, medical laser, optical communication and high-energy physics [1]. Directly pumped mid-IR solid-state lasers have attracted significant attention due to their advantages such as simple system composition, compact size, high efficiency and high output power. Active ions and host materials are both important in obtaining diode laser pumped solid-state lasers.

Rare-earth ions (Tm³⁺, Er³⁺, Ho³⁺ and Dy³⁺) are the preferred active ions for laser emission in the mid-IR spectral range. Tm³⁺, Er³⁺, Ho³⁺ ions have been reported with 2–3 μ m lasing in crystalline or glass hosts such as Tm:YAG [2], Tm:YLF [3], Tm:ZBLAN [4],

Tm:SrF₂ [5], Ho:CaF₂ [6], Ho:YAG [7], Er:SrF₂ [8] and Er:YSGG [9]. With energy transitions corresponding to 2.3–3.4 μm and 4.0–6.2 μm, Dy³⁺ is recognized as an active ion with high potential applications for mid-IR lasers. However, compared with other rare-earth ions, such as Tm³⁺, Er³⁺ and Ho³⁺, laser emissions from Dy³⁺ ion-based solid-state systems are relatively rare. In addition, the intrinsic emission wavelengths of Dy³⁺ include emission band peaks around 2.4, 3.4, 4.3 and 5.4 μm. Owing to the even electron number of 4f electron shells in Dy³⁺ and Stark effects in different crystal fields, a smooth broadband emission spectrum around 2.3–3.4 μm could lead to tunable or ultrafast laser output.

Recently, Dy³⁺ laser has been investigated in fluorozirconate ZBLAN glass fiber with compositions of ZrF₄, BaF₂, LaF₃, AlF₃ and NaF. In 2003, Jackson reported a 2.9 μm CW laser from Dy:ZBLAN with maximum output power of 275 mW and slope efficiency of 4.5% [10]. In 2011, Tsang and El-Taher demonstrated an efficient Dy:ZBLAN fiber lasing around 3 μm with slope efficiency of 23%. However, the output power was limited to 100 mW [11]. In 2016, Majewski et al. reported a Dy:ZBLAN laser at 3.04 μm, with a slope efficiency of 51% and maximum output of 80 mW [12]. In 2018, Woodward et al. successfully obtained watt-level Dy:ZBLAN fiber laser at 3.15 μm with slope efficiency of 73% [13]. In contrast, Dy³⁺-doped crystals are yet to be explored for mid-IR lasers. Currently, the Dy³⁺-doped crystalline host is limited in fluoride and thiogallate crystals such as Dy:BaY₂F₈ [14], Dy:LYF [15], Dy:PbGa₂S₄ [16,17] and Dy:CaGa₂S₄ [18]. Due to superior thermal, mechanical and moisture-proof properties, the Dy³⁺-doped crystalline host is expected to have good performance in the mid-IR spectral range compared with those in ZBLAN fiber.

In this work, a family of CaF₂-SrF₂ crystals doped with Dy(III) was prepared to generate efficient mid-IR emission properties for potential applications in mid-IR lasers. CaF₂-SrF₂ crystal was selected as host material with a molar ratio of 1:1 for Ca/Sr, as inspired by predominant optical properties when doped with rare-earth ions such as Yb³⁺ [19,20]. Meanwhile, CaF₂-SrF₂ possesses low phonon energy, which is of benefit to weaken nonradiative decay from intermediate states to lower ground states in rare-earth ions [21,22]. Moreover, CaF₂-SrF₂ is an azeotrope system, and even the composition ratio of Ca/Sr is different [23,24]. Karimov et al. reported the growth of mixed crystals at the azeotrope point [25].

This research work focuses on crystal growth of Dy:CaF₂-SrF₂ with different Dy³⁺ dopant concentrations. The refractive index and related Sellmeier dispersion formula were obtained in the range of 1.7–11 μm. Optical characterization was conducted in the mid-IR spectral range, followed by the discussions of the energy transfer path in Dy:CaF₂-SrF₂ crystal.

2. Materials and Methods

2.1. Crystal Growth

Dy:CaF₂-SrF₂ crystal boules, with Dy³⁺ concentrations of 5 at.%, 10 at.% and 15 at.%, were fabricated by multicrucible temperature gradient technology (MC-TGT). TGT is a directional solidification technique adapted for the growth of high-temperature crystals [26]. The traditional TGT method allows for one-crucible crystal growth. To enhance growth efficiency, we developed an MC-TGT that allows obtaining multiple crystal boules in the one-growth process [22]. Six crucibles were fixed in the furnace. Benefiting from the azeotrope properties of CaF₂-SrF₂, no crystal seed was used. A stable temperature gradient was then built around the crucible to conduct latent heat and to promote crystallization. The starting materials were CaF₂, SrF₂ and DyF₃ powders with purity higher than 99.995%. The raw materials were mixed according to Ca/Sr molar ratio of 1:1 before placing it in a graphite crucible. Then, 1 wt.% PbF₂ was added to remove oxygen. The melting points of DyF₃, CaF₂ and SrF₂ are 1360 °C, 1420 °C and 1477 °C, respectively. The furnace was insulated for 3 h at 1530 °C while evacuating to 10^{−3} Pa. The cooling rate for crystal growth was set at 1.5 °C/h. After growth, the crucible was cooled to room temperature

at a cooling rate of 20 °C/h. The Dy:CaF₂-SrF₂ crystals were then cut and processed for subsequent tests.

2.2. Characterizations

The segregation coefficient of Dy³⁺ ion in the CaF₂-SrF₂ host was detected by inductively coupled plasma atomic emission spectrometry (ICP-AES). The sample was cut from the initial part of the crystal and then ground into fine powder in an agate mortar. The solvent was a mixture of phosphoric acid and boric acid. After obtaining the weight percentage of Dy³⁺, Ca²⁺ and Sr²⁺ in the solvent, the dopant level of Dy³⁺ was calculated. The segregation coefficient could thus be calculated by dividing the measured dopant value of Dy³⁺ by the theoretical value. The segregation coefficient was measured for the sample adjacent to the initial part of the as-grown crystal boules.

The structure of Dy:CaF₂-SrF₂ crystal was measured by a powder-X-ray diffractometer (P-XRD, RIGAKU TTRIII-18KW, Tokyo, Japan) using a Cu target at room temperature. The scan rate was 3°/min. The raw data from the P-XRD pattern were analyzed to fix the diffraction peak by comparing with the standard Power Diffraction File (PDF) data from Jade software. The diffractograms were gathered by Origin software.

The refractive index in the mid-IR spectral range was characterized using an infrared ellipsometer (J.A. Woollam IR-Vase II, Lincoln, NE, USA). The single crystal along the growth axis was cut with a diameter of 20 mm and a thickness of 1 mm. One surface was polished, while the other surface was kept rough for measurement. The measured data were then analyzed by nonlinear fitting by Origin software to obtain dispersion formula.

The optical quality of as-grown crystal boules was characterized by mid-IR transmission spectra with a sampling step of 2.8 nm (Bruker TENSOR27, Karlsruhe, Germany). Absorption spectra were measured with a UV/vis/NIR spectrophotometer (Varian Cary 5000, Palo Alto, CA, USA) using Xe light as a pump source. Fluorescence spectra were measured with an 808 nm pump source (Edinburg Instruments FLS1000, Livingston, UK) and an InSb detector. As a comparison, a 1320 nm pump source from a pulse generator (Thurlby Thandar Instruments TGP 110, Huntingdon, UK) was used for fluorescence spectra, emitting at 1200–3500 nm, recorded by a digital phosphor oscilloscope with sampling rate of 1.25 GS/s and frequency of 100 MHz (Tektronix TDS 3012C, Beaverton, OR, USA). The fluorescence lifetime measurement was carried out by a computer-controlled transient digitizer decay curve of emission under a pump wavelength of 808 nm. Single crystals with a thickness of 1 mm along the growth axis were polished and then used for the above-mentioned spectroscopic measurements. All measurements were performed at room temperature.

3. Results and Discussion

3.1. Crystal Structure and Optical Quality

The traditional TGT method allows for one-crucible crystal growth. To enhance growth efficiency, we developed an MC-TGT that allows obtaining multiple crystal boules in the one-growth process. Figure 1 shows the obtained Dy:CaF₂-SrF₂ crystal boules up to 20 mm in diameter and 68 mm in length. The as-grown yellow boules are homogeneous without bubbles. The dopants of Dy³⁺ ions are 5 at.%, 10 at.% and 15 at.%. The segregation coefficient of Dy³⁺ ion in 5 at.% Dy:CaF₂-SrF₂ and 15 at.% Dy:CaF₂-SrF₂ is 1.0, while that in 10 at.% Dy:CaF₂-SrF₂ is 0.96. This indicates the high solubility of Dy³⁺ ion in the CaF₂-SrF₂ host lattice.

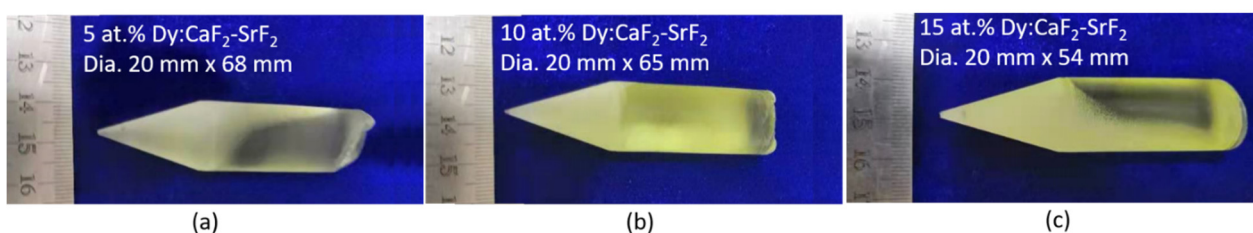


Figure 1. As-grown Dy:CaF₂-SrF₂ crystal boules using MC-TGT. (a) 5at.% Dy; (b) 10at.% Dy; (c) 15at.% Dy.

The method of Archimedes' hydrostatic weighing principle aids in the determination of density following Equation (1).

$$\rho = m_1 \cdot \rho_1 / (m_1 - m_2) \quad (1)$$

Here, m_1 and m_2 are sample weights measured in air and in water, respectively. ρ_1 is the density of water marked as $1 \text{ g}\cdot\text{cm}^{-3}$. ρ is the sample density in air to be determined. The test results are listed in Table 1.

Table 1. Density determination following Archimedes' hydrostatic weighing principle.

Crystals	m_1 (g)	m_2 (g)	ρ (g/cm^3)
5% Dy:CaF ₂ -SrF ₂	12.24010	9.20478	4.03256
10% Dy:CaF ₂ -SrF ₂	14.00670	10.69937	4.23505
15% Dy:CaF ₂ -SrF ₂	13.22491	10.28247	4.49454

Figure 2 gives the measured XRD pattern of Dy:CaF₂-SrF₂ crystal compared with that of pure CaF₂ referring to PDF Number 75-0363 and that of pure SrF₂ referring to PDF Number 06-0262. The main three strongest peaks in CaF₂ are located at 2θ of 28.272° for (111), 47.008° for (200) and 55.764° for (311), while those in SrF₂ are located at 2θ of 26.57° for (111), 44.123° for (200) and 52.273° for (311). In the case of Dy:CaF₂-SrF₂ crystal, the three strongest peaks are located at 2θ of 27.46° , 45.52° and 53.96° . The diffraction angles 2θ of Dy:CaF₂-SrF₂ situates in-between those of CaF₂ and SrF₂. This indicates that Dy:CaF₂-SrF₂ crystal is fluorite structured and crystallizes in the cubic $Fm\bar{3}m$ space group.

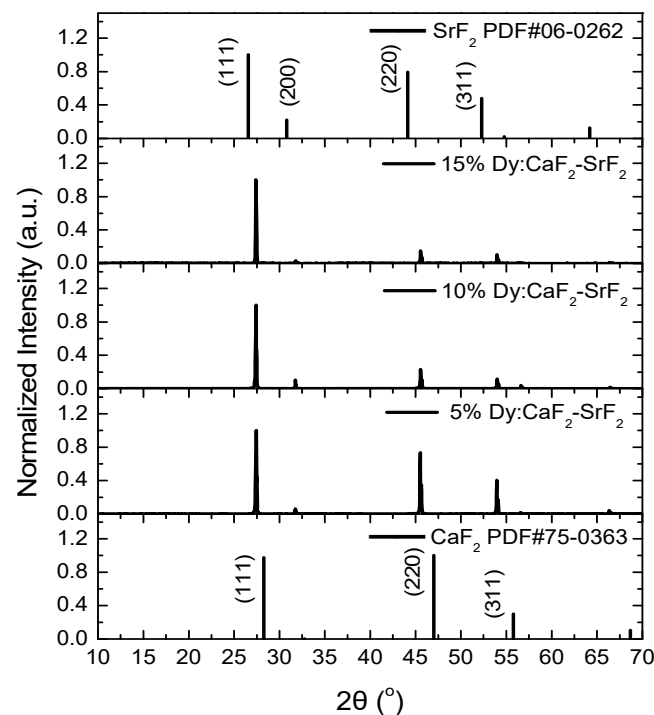


Figure 2. XRD pattern of Dy:CaF₂-SrF₂ crystal.

The optical quality of polished Dy:CaF₂-SrF₂ crystals was characterized by transmission spectra. Figure 3 gives the transmission spectra of Dy:CaF₂-SrF₂ at 2–11 μm . The transmission curves in Figure 3 are based on measured raw data subtracting the background without considering the reflections on both surfaces. It shows that the transmission of all three polished samples is above 90% from 4 to 9 μm . The infrared transmittance cut-off wavelength is around 11 μm . It could be concluded that the crystallinity and optical quality of Dy:CaF₂-SrF₂ crystal boules are good.

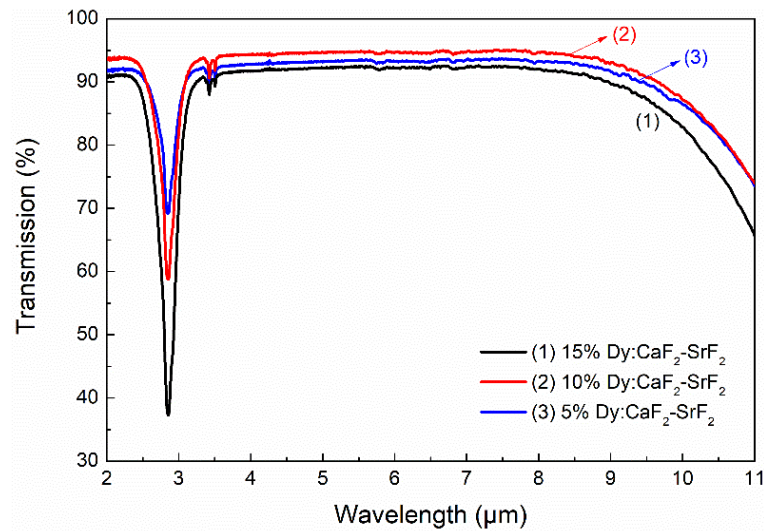


Figure 3. Transmission spectra of Dy:CaF₂-SrF₂ crystals at 2–11 μm.

3.2. Refractive Index in the Mid-IR Spectral Range

Figure 4 gives the refractive index of Dy:CaF₂-SrF₂ in the mid-IR spectral range of 1.7–11 μm. As seen from Figure 4, the refractive index of Dy:CaF₂-SrF₂ increases along with a higher dopant level of Dy³⁺. The Sellmeier dispersion formula is used for nonlinear fitting. The dispersion formula for Dy:CaF₂-SrF₂ with Dy³⁺ dopant levels of 5%, 10% and 15% is thus achieved and described in Equations (2)–(4), respectively. The reduced Chi-square is 2.70×10^{-5} . The adjusted R² is 0.9986.

$$n^2 - 1 = 0.20292 + \frac{0.69272\lambda^2}{\lambda^2 - 0.94855^2} + \frac{0.87102\lambda^2}{\lambda^2 - 60.10^2} + \frac{5.64914\lambda^2}{\lambda^2 - 45.04^2} \quad (2)$$

$$n^2 - 1 = 0.21687 + \frac{0.70758\lambda^2}{\lambda^2 - 0.97111^2} + \frac{1.84394\lambda^2}{\lambda^2 - 70.44^2} + \frac{6.11963\lambda^2}{\lambda^2 - 48.55^2} \quad (3)$$

$$n^2 - 1 = 0.20292 + \frac{0.73684\lambda^2}{\lambda^2 - 0.97075^2} + \frac{2.30876\lambda^2}{\lambda^2 - 69.93^2} + \frac{6.15892\lambda^2}{\lambda^2 - 50.30^2} \quad (4)$$

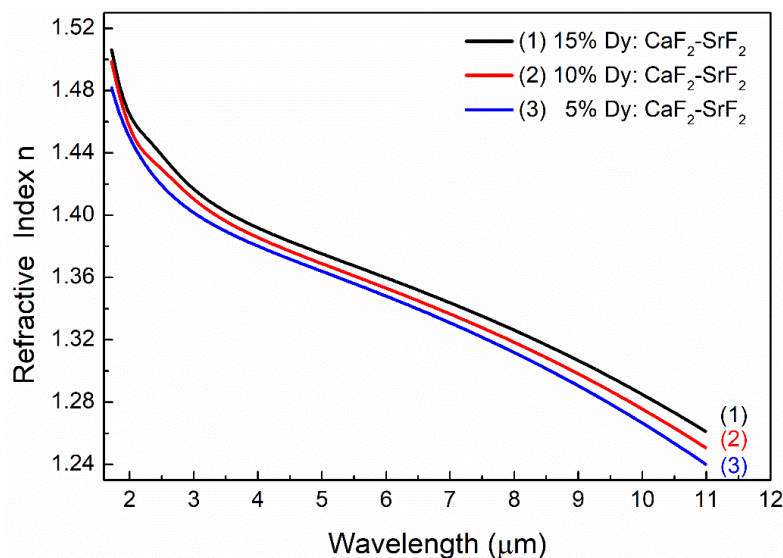


Figure 4. Refractive index of Dy:CaF₂-SrF₂ in the mid-IR spectral range of 1.7–11 μm.

3.3. Absorption and Emission Spectra

Figure 5 shows the room-temperature absorption spectra in the spectral range of 650–1900 nm and the assignment of energy level in Dy:CaF₂-SrF₂ crystals. The assignment of energy level could refer to that in Dy:BaY₂F₈ [27]. In the mid-IR region, Dy³⁺ ions show broad absorption bands in 5% Dy:CaF₂-SrF₂ crystal peaks at 804 nm, 907 nm, 1092 nm, 1276 nm and 1714 nm corresponding to absorption coefficients of 2.12 cm⁻¹, 2.69 cm⁻¹, 4.04 cm⁻¹, 2.54 cm⁻¹ and 1.18 cm⁻¹, respectively. In the case of 10% Dy:CaF₂-SrF₂ crystal, the absorption coefficients are 3.56 cm⁻¹, 4.46 cm⁻¹, 7.08 cm⁻¹, 4.47 cm⁻¹ and 2.02 cm⁻¹, corresponding to absorption band peaks at 804 nm, 908 nm, 1093 nm, 1273 nm and 1716 nm. For 15% Dy:CaF₂-SrF₂ crystal, it gives the strongest absorption coefficients of 6.06 cm⁻¹, 7.56 cm⁻¹, 12.71 cm⁻¹, 8.25 cm⁻¹ and 3.63 cm⁻¹, corresponding to absorption band peaks at 804 nm, 907 nm, 1094 nm, 1277 nm and 1716 nm. The absorption band peaks at 1308 nm and 1720 nm correspond to energy level transitions of ⁶H_{15/2}→⁶H_{9/2}, ⁶F_{11/2} and ⁶H_{15/2}→⁶H_{11/2} in Dy³⁺ ion. With the increase in Dy³⁺ ion dopant levels from 5% to 15%, the absorption coefficient becomes 2.8–3.3 times stronger. Broad absorption bands are profitable in increasing the diode-pumping efficiency, as laser diodes typically emit in a narrow spectral range and present a thermal shift in the peak wavelength.

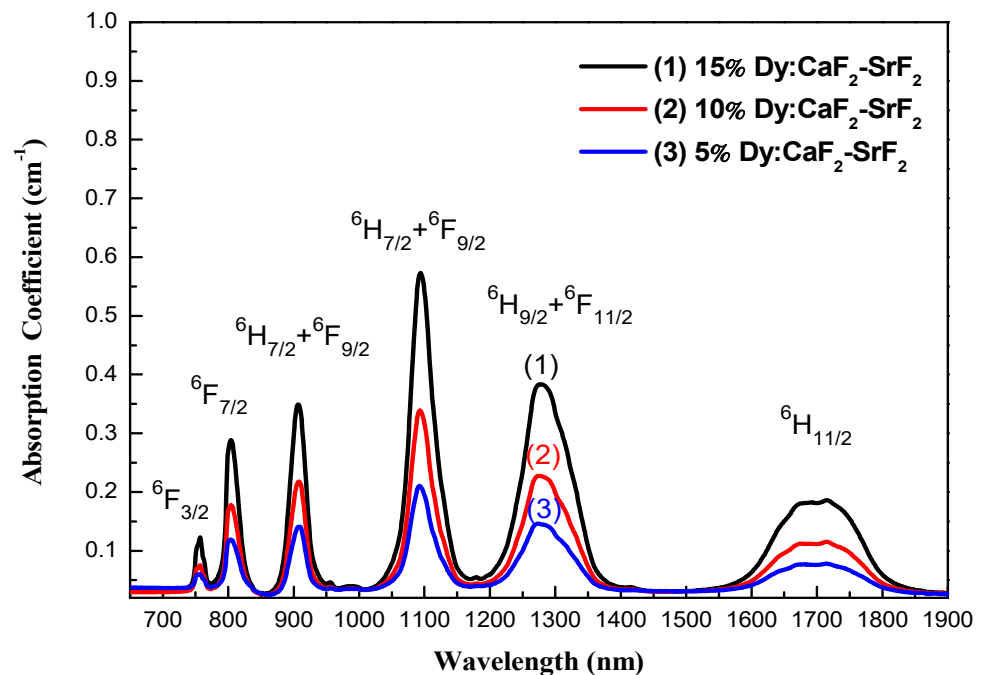


Figure 5. Absorption coefficient of Dy:CaF₂-SrF₂ crystal at 650–1900 nm.

Table 2 gives the calculated absorption cross-section of Dy³⁺ according to the expression $\sigma_{abs} = \alpha/N$. Here, α is the absorption coefficient of Dy³⁺. N is the concentration of Dy³⁺ ions with 1.21×10^{21} ion·cm⁻³, 2.42×10^{21} ion·cm⁻³ and 4.03×10^{21} ion·cm⁻³ in 5% Dy:CaF₂-SrF₂, 10% Dy:CaF₂-SrF₂ and 15% Dy:CaF₂-SrF₂, respectively.

Table 2. Absorption cross-section (σ_{abs}) of Dy³⁺ ions at 650–1900 nm.

Crystal	σ_{abs} ($\times 10^{-20}$ cm ²)			
	804 nm	907 nm	1094 nm	1287 nm
5% Dy:CaF ₂ -SrF ₂	0.176	0.223	0.335	0.211
10% Dy:CaF ₂ -SrF ₂	0.147	0.184	0.293	0.185
15% Dy:CaF ₂ -SrF ₂	0.150	0.187	0.315	0.205

Figure 6 shows the emission spectra and peak assignment of Dy:CaF₂-SrF₂ crystal in the mid-IR range under excitation wavelengths of 808 nm and 1320 nm. In the case of using a pump wavelength of 1320 nm, as shown in Figure 6a, the fluorescence band peak at 1970 nm, corresponding to the energy level transition from ⁶H_{9/2} + ⁶F_{11/2} to ⁶H_{13/2} [16], was detected with an intensity variation in the order of the Dy³⁺ doping concentration. The strongest fluorescence intensity appears in 5% Dy:CaF₂-SrF₂, while the lowest fluorescence intensity appears in 15% Dy:CaF₂-SrF₂. It is interesting to note that the intensity of the fluorescence band peak at 2882 nm is not affected by the Dy³⁺ doping concentration.

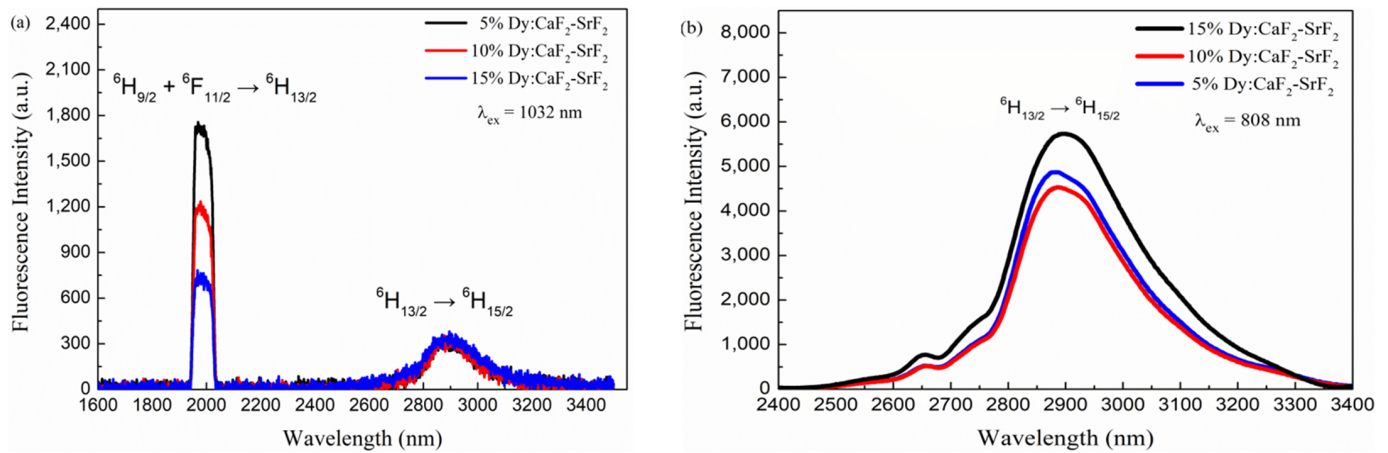


Figure 6. Emission spectra of Dy:CaF₂-SrF₂ crystal under different pump source. (a) 1320 nm pump; (b) 808 nm pump.

Figure 6b shows the emission spectra by using an excitation wavelength of 808 nm. The emission intensity of 10% Dy:CaF₂-SrF₂ is the lowest, while that of 15% Dy:CaF₂-SrF₂ is the highest. In order to illustrate the mid-IR fluorescence bands, nonlinear fittings for multiple peaks are used in the form of the Lorentz function. Taking 15% Dy:CaF₂-SrF₂ for example, the full width at half maximum (FWHM) is 267 nm for the emission band peak at 2919 nm, corresponding to the energy level transition from ⁶H_{13/2} to ⁶H_{15/2} of Dy³⁺ ion. In the case of Dy:CaF₂-SrF₂ with Dy³⁺ dopant levels of 10% and 5%, the values of FWHM are both 237 nm. All emission bands peak at 2913 nm.

Figure 7 gives the measured fluorescence lifetime curves for the energy transfer channel ⁶H_{13/2} → ⁶H_{15/2} of Dy³⁺ ions in Dy:CaF₂-SrF₂ crystals. The obtained fluorescence lifetime curves are processed with nonlinear fitting according to the second-order exponential formula (ExpDec2), as described in Equation (5).

$$y = A_0 + A_1 e^{-\frac{\tau}{t_1}} + A_2 e^{-\frac{\tau}{t_2}} \quad (5)$$

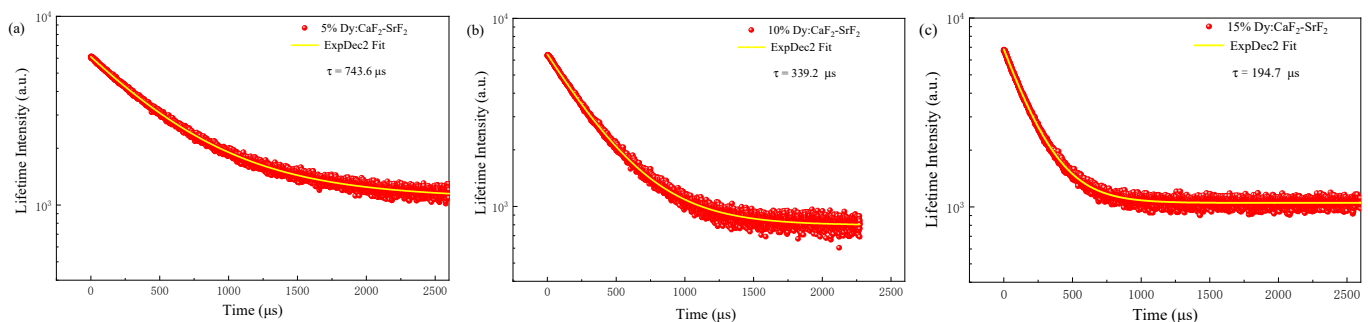


Figure 7. Measured and nonlinear fitted fluorescence lifetime curves in Dy:CaF₂-SrF₂. (a) 5% Dy; (b) 10% Dy; (c) 15% Dy.

Here, A_0 , A_1 , A_2 , t_1 and t_2 are constant values that could be obtained from the fitting results. Accordingly, the second-order exponential formula for Dy:CaF₂-SrF₂ with various

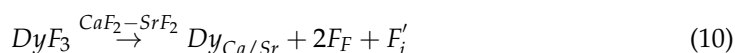
Dy³⁺ dopant levels is thus written in Equations (6)–(8). The average fluorescence lifetime could be obtained from Equation (9). The fluorescence lifetimes are calculated as 743.6 μs, 339.2 μs and 194.7 μs for Dy:CaF₂-SrF₂ with Dy³⁺ dopant levels of 5%, 10% and 15%, respectively. The reduction of fluorescence lifetime along with a higher Dy³⁺ concentration could be attributed to the increase in interstitial fluoride ions. The mechanism could be described in the defect reaction equation as shown in Equation (10). It would be interesting to investigate the mechanism of enhancing fluorescence intensity while maintaining lifetime in future work.

$$y = 1046.495 + 331.646e^{-\frac{\tau}{1723.164}} + 4722.538e^{-\frac{\tau}{512.166}} \quad (6)$$

$$y = 793.798 + 5605.837e^{-\frac{\tau}{339.964}} + 60.970e^{-\frac{\tau}{104.241}} \quad (7)$$

$$y = 1050.882 + 2892.258e^{-\frac{\tau}{194.744}} + 2892.258e^{-\frac{\tau}{194.744}} \quad (8)$$

$$\tau = \frac{A_1 t_1^2 + A_2 t_2^2}{A_1 t_1 + A_2 t_2} \quad (9)$$



4. Summary

This paper concerns the important issue of novel emissive materials for laser applications in the significant mid-IR range. Dy³⁺-doped CaF₂-SrF₂ crystals with fluorite structure and cubic *Fm* $\bar{3}$ *m* space group were synthesized by MC-TGT. The crystallographic site concentrations were up to 4.034×10^{21} ions·cm⁻³ in 15 at.% Dy:CaF₂-SrF₂. The optical transmission of Dy:CaF₂-SrF₂ crystal reached over 90% with a sample thickness of 1.0 mm. The Sellmeier dispersion formula for 1.7–11 μm was obtained from the refractive index. The strongest absorption coefficients of 6.06 cm⁻¹, 7.56 cm⁻¹, 12.71 cm⁻¹, 8.25 cm⁻¹ and 3.63 cm⁻¹ were obtained in 15% Dy:CaF₂-SrF₂ crystal corresponding to absorption band peaks at 804 nm, 907 nm, 1094 nm, 1277 nm and 1716 nm. The value of FWHM was 267 nm for the emission band peak at 2919 nm in 15% Dy:CaF₂-SrF₂ under an excitation wavelength of 808 nm. The fluorescence lifetime in 5% Dy:CaF₂-SrF₂ was 3.8 times longer than that in 15% Dy:CaF₂-SrF₂. Further research work will focus on the enhancement of lifetime while maintaining strong emission in the mid-IR spectral range.

Author Contributions: Methodology—W.C.; formal analysis—J.Z., H.L. (Hui Lin), Y.X., Y.L. and R.Y.; investigation—H.L. (Haifeng Lu), Y.W., H.L. (Hui Lin), R.Y., J.L. and Y.X.; validation—F.R. and X.X.; funding acquisition—L.S.; supervision—L.Z.; writing—original draft preparation—W.C. and J.Z.; writing—review and editing—L.Z., F.R. and L.S. All authors have read and agreed to the published version of the manuscript.

Funding: This research was funded by National Natural Science Foundation of China, Grant Number U1830104; Opening Project of the State Key Laboratory of Transparent Opto-functional Inorganic Materials, Chinese Academy of Science, Grant Number KLTOIM202001; Yunnan Fundamental Research Projects, Grant Number 202101AT070162; Yunnan University First-class University Construction Project, Grant Number C176220100155; Innovative entrepreneurial training for Yunnan College Students, Grant Number 202010673075.

Data Availability Statement: Not applicable.

Acknowledgments: The authors acknowledge the experimental support from Shaohua Wu and Huajin Wang.

Conflicts of Interest: The authors declare no conflict of interest.

References

- Xue, Y.Y.; Xu, X.D.; Su, L.B.; Xu, J. Research Progress of Mid-infrared Laser Crystals. *J. Synth. Cryst.* **2020**, *49*, 1347–1360.
- Cao, D.; Peng, Q.; Du, S.; Xu, J.; Guo, Y.; Yang, J.; Bo, Y.; Zhang, J.; Cui, D.; Xu, Z. A 200 W diode-side-pumped CW 2 μm Tm:YAG laser with water cooling at 8 °C. *Appl. Phys. B* **2011**, *103*, 83–88. [[CrossRef](#)]

3. Wang, S.Q.; Huang, H.T.; Chen, H.W.; Liu, X.; Liu, S.D.; Xu, J.L.; Shen, D.Y. High efficiency nanosecond passively Q-switched 2.3 μm Tm:YLF laser using a ReSe₂-based saturable output coupler. *OSA Contin.* **2019**, *2*, 1676–1682. [[CrossRef](#)]
4. Lancaster, D.G.; Gross, S.; Ebendorff-Heidepriem, H.; Fuerbach, A.; Withford, M.J.; Monro, T.M. 2.1 μm waveguide laser fabricated by femtosecond laser direct-writing in Ho³⁺, Tm³⁺:ZBLAN glass. *Opt. Lett.* **2012**, *37*, 996–998. [[CrossRef](#)] [[PubMed](#)]
5. Sottile, A.; Damiano, E.; Rabe, M.; Bertram, R.; Klimm, D.; Tonelli, M. Widely tunable, efficient 2 μm laser in monocrystalline Tm³⁺:SrF₂. *Opt. Express* **2018**, *26*, 5368–5380. [[CrossRef](#)] [[PubMed](#)]
6. Duan, X.M.; Shen, Y.J.; Zhang, Z.; Su, L.B.; Dai, T.Y. A passively Q-switching of diode-pumped 2.08 μm Ho:CaF₂ laser. *Infrared Phys. Technol.* **2019**, *103*, 103071. [[CrossRef](#)]
7. Duan, X.M.; Shen, Y.J.; Yao, B.Q.; Wang, Y.Z. A 106 W Q-switched Ho:YAG laser with single crystal. *Optik* **2018**, *169*, 224–227. [[CrossRef](#)]
8. Fan, M.Q.; Li, T.; Zhao, J.; Zhao, S.Z.; Li, G.Q.; Yang, K.J.; Su, L.B.; Ma, H.Y.; Kränkel, C. Continuous wave and ReS₂ passively Q-switched Er:SrF₂ laser at $\sim 3 \mu\text{m}$. *Opt. Lett.* **2018**, *43*, 1726–1729. [[CrossRef](#)]
9. Shen, B.J.; Kang, H.X.; Chen, P.; Liang, J.; Ma, Q.; Fang, J.; Sun, D.L.; Zhang, Q.L.; Yin, S.T.; Yan, X.P.; et al. Performance of continuous-wave laser-diode side-pumped Er:YSGG slab lasers at 2.79 μm . *Appl. Phys. B* **2015**, *121*, 511–515. [[CrossRef](#)]
10. Jackson, S.D. Continuous wave 2.9 μm dysprosium-doped fluoride fiber laser. *Appl. Phys. Lett.* **2003**, *83*, 1316–1318. [[CrossRef](#)]
11. Tsang, Y.H.; El-Taher, A.E. Efficient lasing at near 3 μm by a Dy-doped ZBLAN fiber laser pumped at $\sim 1.1 \mu\text{m}$ by an Yb fiber laser. *Laser Phys. Lett.* **2011**, *8*, 818–822. [[CrossRef](#)]
12. Majewski, M.R.; Jackson, S.D. Highly efficient mid-infrared dysprosium fiber laser. *Opt. Lett.* **2016**, *41*, 2173–2176. [[CrossRef](#)] [[PubMed](#)]
13. Woodward, R.I.; Majewski, M.R.; Bharathan, G.; Hudson, D.D.; Fuerbach, A.; Jackson, S.D. Watt-level dysprosium fiber laser at 3.15 μm with 73% slope efficiency. *Opt. Lett.* **2018**, *43*, 1471–1474. [[CrossRef](#)] [[PubMed](#)]
14. Djeu, N.; Hartwell, V.E.; Kaminskii, A.A.; Butashin, A.V. Room-temperature 3.4- μm Dy:BaYb₂F₈ laser. *Opt. Lett.* **1997**, *22*, 997–999. [[CrossRef](#)]
15. Barnes, N.P.; Allen, R.E. Room temperature Dy:YLF laser operation at 4.34 μm . *IEEE J. Quantum Electron.* **1991**, *27*, 277–282. [[CrossRef](#)]
16. Jelinkova, H.; Doroshenko, M.E.; Osiko, V.V.; Jelínek, M.; Šulc, J.; Němec, M.; Vyhlídal, D.; Badikov, V.V.; Badikov, D.V. Dysprosium thiogallate laser: Source of mid-infrared radiation at 2.4, 4.3, and 5.4 μm . *Appl. Phys. A* **2016**, *122*, 738. [[CrossRef](#)]
17. Jelínková, H.; Doroshenko, M.E.; Jelínek, M.; Šulc, J.; Osiko, V.V.; Badikov, V.V.; Badikov, D.V. Dysprosium-doped PbGa₂S₄ laser generating at 4.3 μm directly pumped by 1.7 μm laser diode. *Opt. Lett.* **2013**, *38*, 3040–3043. [[CrossRef](#)]
18. Nostrand, M.C.; Page, R.H.; Payne, S.A.; Krupke, W.F.; Schunemann, P.G. Room-temperature laser action at 4.3–4.4 μm in CaGa₂S₄:Dy³⁺. *Opt. Lett.* **1999**, *24*, 1215–1217. [[CrossRef](#)]
19. Zhang, F.; Zhu, H.T.; Liu, J.; He, Y.F.; Jiang, D.P.; Tang, F.; Su, L.B. Tunable Yb:CaF₂-SrF₂ laser and femtosecond mode-locked performance based on semiconductor saturable absorber mirrors. *Appl. Opt.* **2016**, *55*, 8359–8362. [[CrossRef](#)] [[PubMed](#)]
20. Jiang, B.B.; Zheng, L.H.; Jiang, D.P.; Yin, H.D.; Zheng, J.G.; Yang, Q.H.; Cheng, G.F.; Su, L.B. Growth and optical properties of ytterbium and rare earth ions codoped CaF₂-SrF₂ eutectic solid-solution (RE = Y³⁺, Gd³⁺, La³⁺). *J. Rare Earths* **2021**, *39*, 390–397. [[CrossRef](#)]
21. Ma, F.; Su, F.; Zhou, R.; Ou, Y.; Xie, L.; Liu, C.; Jiang, D.; Zhang, Z.; Wu, Q.; Su, L.; et al. The defect aggregation of RE³⁺ (RE = Y, La \sim Lu) in MF₂ (M = Ca, Sr, Ba) fluorites. *Mater. Res. Bull.* **2020**, *125*, 110788. [[CrossRef](#)]
22. Ruan, F.F.; Yang, L.; Hu, G.; Wang, A.M.; Xue, Y.Y.; Yang, L.L.; Wang, Z.X.; Wu, S.H.; He, Z.L. Luminescence Properties of Dy³⁺ Doped Lanthanum Fluoride Crystal by Multi-crucible Temperature Gradient Technology. *Chin. J. Lumin.* **2021**, *42*, 158–164. [[CrossRef](#)]
23. Renaud, E.; Robelin, C.; Heyrman, M.; Chartrand, P. Thermodynamic evaluation and optimization of the (LiF + NaF + KF + MgF₂ + CaF₂ + SrF₂) system. *J. Chem. Thermodyn.* **2009**, *41*, 666–682. [[CrossRef](#)]
24. Klimm, D.; Rabe, M.; Bertram, R.; Uecker, R.; Parthier, L. Phase diagram analysis and crystal growth of solid solutions Ca_{1-x}Sr_xF₂. *J. Cryst. Growth* **2008**, *310*, 152–155. [[CrossRef](#)]
25. Karimov, D.N.; Komar'kova, O.N.; Sorokin, N.I.; Bezhanov, V.A.; Chernov, S.P.; Popov, P.A.; Sobolev, B.P. Growth of congruently melting Ca_{0.59}Sr_{0.41}F₂ crystals and study of their properties. *Crystallogr. Rep.* **2010**, *55*, 518–524. [[CrossRef](#)]
26. Xu, J.W.; Zhou, Y.Z.; Zhou, G.Q.; Xu, K.; Deng, P.Z.; Xu, J. Growth of large-sized sapphire boules by temperature gradient technique (TGT). *J. Cryst. Growth* **1998**, *193*, 123–126.
27. Johnson, L.F.; Guggenheim, H.J. Laser emission at 3 μm from Dy³⁺ in BaY₂F₈. *Appl. Phys. Lett.* **1973**, *23*, 96–98. [[CrossRef](#)]